Sigma J Eng & Nat Sci 35 (2), 2017, 227-238

Sigma Journal of Engineering and Natural Sciences
Sigma Mühendislik ve Fen Bilimleri Dergisi

Research Article

INFRARED DRYING CHARACTERISTICS OF JERUSALEM ARTICHOKE SLICES

İbrahim DOYMAZ*

Department of Chemical Engineering, Yildiz Technical University, Esenler-ISTANBUL

Received: 26.08.2016 Revised: 08.02.2017 Accepted: 25.02.2017

ABSTRACT

In this study, drying characteristics of Jerusalem artichoke slices were investigated by using infrared technique. The Jerusalem artichoke slices were dried at 62, 74, 88, 104 and 125 W infrared power levels. An increase in the infrared power resulted in a significant reduction in the drying time. Lewis, Henderson and Pabis, Logarithmic, Midilli and Kucuk, and Wang and Singh models were used to fit experimental data. The Midilli and Kucuk model has been determined to be the best model that represents the experimental data. Effective moisture diffusivity values ranged from 4.81×10^{-10} m^2/s to 1.97×10^{-9} m^2/s, and increased with the increase in infrared power. The activation energy was calculated as 6.74 kW/kg.
Keywords: Activation energy, effective moisture diffusivity, infrared drying, Jerusalem artichoke, mathematical modelling.

1. INTRODUCTION

Jerusalem artichoke (*Helianthus tuberosus* L.) produces fleshy underground tubers rich in inulin and related carbohydrates. The Jerusalem artichoke is called the sunroot, sunchoke, earth apple, or topinumbour [1]. Obtained from Jerusalem artichoke tubers useful components intended for use as raw materials for foods. Powder artichoke (Jerusalem artichoke flour) contains complex carbohydrate components, represented mainly polysaccharide nature inulin (up to 82%), proteins (up to 7%), fat (0.3-0.7%), vitamins (B1, B2, and C), pectin (10%), fiber (7%), organic acids, macro- and trace elements [2]. For long term storage of food products there are various changes (microbiological, enzymatic and biochemical). As a result, the products may be damaged. To inhibit microbial growth and enzymatic activity are widely used natural or artificial drying process. Therefore, the Jerusalem artichokes should be dried for storage, handling and processing.

Drying, which is the process of removal of most of the moisture present in the food is the oldest preservation method applied since ancient times [3]. Drying of agricultural and food products is needed for easy handling, safe preservation and longer storage, and reduction in cost of transportation. This process generally involves removal of water by application of heat. Improper drying may lead to irreversible damages to product quality, high energy and time consumption, unseasonable charges, etc [4]. Drying of agricultural products can be performed

* Corresponding Author/Sorumlu Yazar: e-mail/e-ileti: doymaz@yildiz.edu.tr, tel: (212) 383 47 48

using different methods, including traditional and industrial drying. Infrared drying has gained popularity as an alternative drying method for obtaining high quality dried fruits, vegetables and grains [5]. Infrared radiation technology offers some advantages over conventional drying under similar drying conditions. They may include decreased drying time, high energy efficiency, high quality finished products, and uniform temperature in the product [6-8]. Infrared radiation energy is transferred from the heating element to the product surface without the surrounding air. The radiation impinges on the exposed material and penetrates through it, and then, it is converted to sensible heat [5]. Various agricultural products have been successfully dried by the infrared application and/or by a combined infrared-assisted convection process [5,6,8-11]. However, the infrared drying process of Jerusalem artichoke has not been reported in literature. The main objectives of this study were to investigate the effect of infrared power on drying and color characteristics, fit the experimental data to five thin-layer drying models, and compute effective moisture diffusivity and activation energy of Jerusalem artichokes.

2. MATERIAL AND METHODS

2.1. Raw Material

Jerusalem artichoke samples were purchased from a local market in Istanbul. They were packed into plastic bags and stored in a refrigerator (Arcelik 1050T, Eskisehir, Turkey) at 4°C prior to use. Before the drying process, the Jerusalem artichokes were cut into slices of 5 mm thickness with a mechanical cutter. The initial moisture content of Jerusalem artichoke was determined 75.96%, w.b. (3.1597 kg water/kg dry matter, d.b.).

2.2. Experimental Procedure

Drying experiments were carried out in a moisture analyzer (Snijders Moisture Balance, Snijders b.v., Tilburg, Holland). The experiments were carried out infrared power levels of 62, 75, 88, 104 and 125 W. Before the drying process, the samples were separated evenly and spread homogeneously over the pan. The power level was set from the control unit of the equipment. Approximately 25±0.2 g of sample was put into the dryer after weighing. Moisture loss was recorded at 15 min intervals during drying. A digital balance (Mettler-Toledo AG, Grefensee, Switzerland, model BB3000) with 0.1 g accuracy was employed in recording the sample weight. The drying process was continued until the moisture content remaining in the sample was about 0.10±0.01 kg water/kg dry matter (d.b.). The dried product was cooled and packaged in low-density polyethylene bags and then heat-sealed and stored in incubators at ambient temperature. The experiments were run in triplicate and the average moisture content was used to draw the drying curves.

2.3. Mathematical Modelling

Five semi-theoretical models (Table 1) were selected to describe the drying behaviour of the samples. The moisture content (*M*), moisture ratio (*MR*) and drying rate (*DR*) of Jerusalem artichokes were calculated using the following equations:

$$M = \frac{W - W_1}{W_1} \tag{1}$$

$$MR = \frac{M_t - M_e}{M_0 - M_e} \tag{2}$$

$$DR = \frac{M_t - M_{t+dt}}{dt} \tag{3}$$

Table 1. Mathematical models applied to the drying curves and statistical parameters

Model name	*Model*	*p (W)*	R^2	*P*	χ^2	*RMSE*
Lewis [12]	$MR = \exp(-kt)$	62	0.9834	30.9372	0.001491	0.135410
		74	0.9564	52.1524	0.005089	0.195356
		88	0.9539	48.6634	0.006067	0.182314
		104	0.9761	43.2458	0.003171	0.106402
		125	0.9619	60.4606	0.005722	0.139133
Henderson and Pabis [13]	$MR = a\exp(-kt)$	62	0.9874	27.2665	0.001201	0.112902
		74	0.9684	44.9784	0.004104	0.175146
		88	0.9656	41.8062	0.005174	0.174608
		104	0.9799	39.6342	0.003189	0.109560
		125	0.9667	56.2311	0.006238	0.145783
Logarithmic [14]	$MR = a\exp(-kt) + c$	62	0.9989	3.9946	0.000105	0.033986
		74	0.9958	11.7793	0.000607	0.050550
		88	0.9874	21.3998	0.002198	0.094769
		104	0.9956	13.3092	0.000868	0.049436
		125	0.9908	26.0585	0.002298	0.073976
Midilli and Kucuk [15]	$MR = a\exp(-kt^n) + b$	62	0.9991	2.7351	0.000094	0.028921
		74	0.9988	5.6748	0.000187	0.032685
		88	0.9990	3.5777	0.000199	0.024625
		104	0.9993	3.0891	0.000172	0.017937
		125	0.9999	1.2325	0.000022	0.005572
Wang and Singh [16]	$MR = 1 + at + bt^2$	62	0.9971	8.2944	0.000268	0.057947
		74	0.9954	10.1765	0.000585	0.045250
		88	0.9881	15.0946	0.001789	0.076935
		104	0.9973	4.7205	0.000420	0.030364
		125	0.9932	16.0817	0.001263	0.051411

a, b, c, k, n empirical constants and coefficients in the drying models

where *M* is the moisture content (kg water/kg dry matter), *W* is the weight of sample (kg), W_1 is the dry matter content of sample (kg), and t is the drying time (min). M_0, M_e, M_t *and* M_{t+dt} are the initial moisture content, the equilibrium moisture content, the moisture content at t and $t+dt$ (kg water/kg dry matter), respectively. As the M_e is very small compared to M_0 and M_t values, the M_e can be neglected and *MR* can be expressed as M_t/M_0 [8,16].

2.4. Data Analysis

Experimental data were analyzed using the Statistica 8.0.550 (StatSoft Inc., USA) software package. The parameters of the models in Table 1 were estimated using a non-linear regression procedure based on the Levenberg-Marquardt algorithm. The fitting quality of the experimental data to all models was evaluated using the coefficient of determination (R^2), mean relative percent error (P), reduced chi-square (χ^2) and root mean square error (RMSE). The results were subjected to analysis variance (ANOVA). Differences between the media analyzed using the least significant difference test with a confidence interval of 95% ($p<0.05$). The R^2, P, χ^2 and RMSE were calculated from the following formulas:

$$R^2 = 1 - \frac{\sum_{i=1}^{N}\left(MR_{pre,i} - MR_{\exp,i}\right)^2}{\sum_{i=1}^{N}\left(\overline{MR}_{pre} - MR_{\exp,i}\right)^2} \tag{4}$$

$$P = \frac{100}{N}\sum_{i=1}^{N}\frac{|MR_{\exp,i} - MR_{pre,i}|}{MR_{\exp,i}} \tag{5}$$

$$\chi^2 = \frac{\sum_{i=1}^{N}\left(MR_{\exp,i} - MR_{pre,i}\right)^2}{N - z} \tag{6}$$

$$RMSE = \left[\frac{1}{N}\sum_{i=1}^{N}(MR_{pre,i} - MR_{\exp,i})^2\right]^{1/2} \tag{7}$$

where $MR_{exp,i}$ and $MR_{pre,i}$ are the experimental and predicted dimensionless moisture ratios, respectively; N is the number of observations; z is the number of constants. A higher R^2 value and lower P, χ^2 and $RMSE$ values indicate a better fit [14,17].

2.5. Calculation of Effective Moisture Diffusivity

Fick's second law of diffusion equation was used to fit the experimental drying data for the determination of effective moisture diffusivity coefficients.

$$\frac{\partial M}{\partial t} = D_{eff}\frac{\partial^2 M}{\partial x^2} \tag{8}$$

where M is the moisture content (kg water/kg dry matter), t is the drying time (s), and D_{eff} is the effective moisture diffusivity (m^2/s). Equation (8) can be used to determine the moisture ratio in terms of infinite series by giving the analytical solutions for various regularly shaped bodies, such as rectangular, cylindrical, and spherical shapes, with the appropriate initial and boundary conditions shown as follows:

$$\begin{aligned} &t = 0, \quad 0 < x < L, \quad && M = M_0 \\ &t > 0, \quad x = 0, && \frac{\partial M}{\partial t} = 0 \\ &t > 0, \quad x = L, && M = M_0 \end{aligned} \tag{9}$$

The present case was considered of slab geometry, and then the first boundary condition states that moisture is initially uniformly distributed throughout the sample. The second implies that the mass transfer is symmetric with respect to the centre of the slab. The third condition states that the surface moisture content of the samples instantaneously reaches equilibrium with the conditions of surroundings air [18].

The solution of diffusion Eq. (8) for slab geometry is solved by Crank [19] and supposed uniform initial moisture distribution, negligible external resistance, constant temperature and diffusivity, and negligible shrinkage:

$$MR = \frac{8}{\pi^2}\sum_{n=0}^{\infty}\frac{1}{(2n+1)^2}\exp\left(-\frac{(2n+1)^2\pi^2 D_{eff}t}{4L^2}\right) \tag{10}$$

where D_{eff} is the effective moisture diffusivity (m^2/s), L is the half thickness of the slab (m), and n is the positive integer. Eq. (10) can be further simplified to only the first term of the series and expressed in a logarithmic form for long drying periods:

$$\ln(MR) = \ln\left(\frac{8}{\pi^2}\right) - \left(\frac{\pi^2 D_{eff}t}{4L^2}\right) \tag{11}$$

The effective moisture diffusivity was calculated from the slope *(K)* of a straight line, plotting experimental drying data in terms of *ln (MR)* versus *time* according to Eq. (11).

$$K = \frac{\pi^2 D_{eff}}{4L^2} \tag{12}$$

2.6. Estimation of Activation Energy

Temperature was not a directly measurable quantity during the infrared power drying process used in this study. The activation energy can be calculated using the modified form of the Arrhenius equation, as derived by Dadali and Ozbek [20], which shows the relationship of the sample weight to the effective moisture diffusivity and the infrared power.

$$\mathrm{D_{eff}} = \mathrm{D_0} \exp\left(-\frac{E_a m}{p}\right) \tag{13}$$

where D_0 is the pre-exponential factor of Arrhenius equation (m^2/s), E_a is the activation energy (W/kg), p is the infrared output power (W), and m is the mass of raw sample (kg).

2.7. Color

The colour values of the fresh and dried samples subjected to infrared powers between 62 and 125 W powers were evaluated using a hand-held tristimulus colorimeter (Chroma Meter-CR-400 from Konica Minolta, Osaka, Japan). The colour brightness coordinate L measures the whiteness value of a colour and ranges from black at 0 to white at 100. The chromaticity coordinate a measures red when positive and green when negative, and the chromaticity coordinate b measures yellow when positive and blue when negative. For the colour determinations, five measurements were done, and the average values were calculated for each set of Jerusalem artichoke slices, fresh and dried at each infrared power.

3. RESULTS AND DISCUSSION

3.1. Analysis of Drying Curves

The effect of infrared power on moisture content and drying time is shown in Figure 1. The infrared power had a significant effect on the moisture content of the Jerusalem artichoke slices, as expected. It is observed that in infrared drying, an increase in the power level resulted in a decrease at drying time where the required time to reach the final moisture content at the power levels of 62, 74, 88, 104, and 125 W, were about 270, 150, 120, 90 and 75 min, respectively. The average drying rates increased 3.6 times as infrared power increased from 62 W to 125 W. In fact, at higher infrared powers, more heat is generated within the material leading to more vapour pressure differences between the centre and surface of the product and consequently, increases the drying rate. This observation agrees well with the results reported in the literature for infrared drying of different products such as onion [7], red pepper [21], and spinach leaves [22].

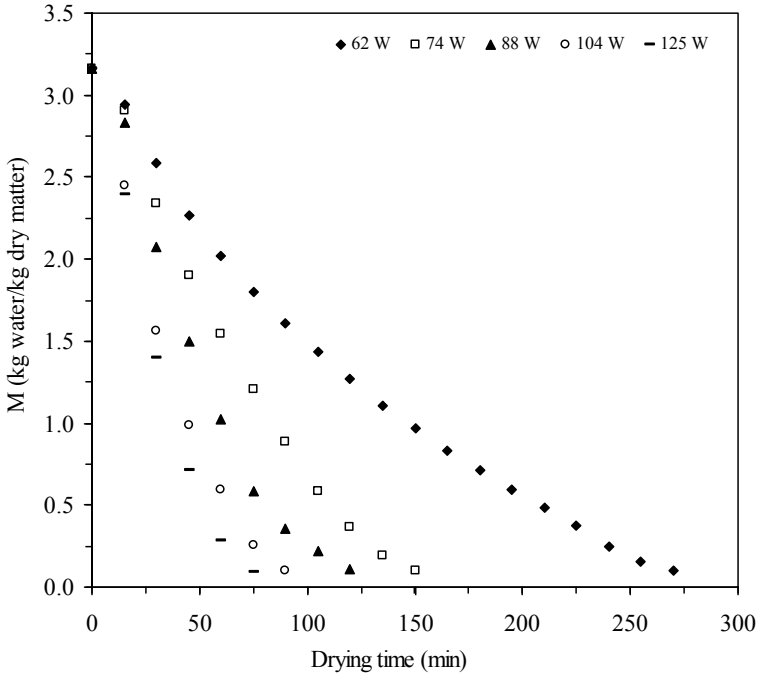

Figure 1. Moisture content during drying time at different infrared powers

3.2. Drying Rate

The drying rate curves of Jerusalem artichoke slices are shown in Figure 2. It is clear that the drying rate decreases continuously with moisture content. The drying rates were higher in the beginning of the process, and then decreased with a decrease in moisture content of the samples. The reason for the decrease in drying rate might be due to a reduction in the porosity of samples caused by shrinkage with advancement, which increased the resistance to movement of water leading to further fall in drying rates [23]. This observation is in agreement with previous studies on infrared drying of foodstuffs [24,25]. Jerusalem artichoke did not exhibit a constant drying rate period and all the drying operations are seen to occur in the falling drying rate period. These results are in good agreement with those in earlier studies of various vegetables [5,10,22].

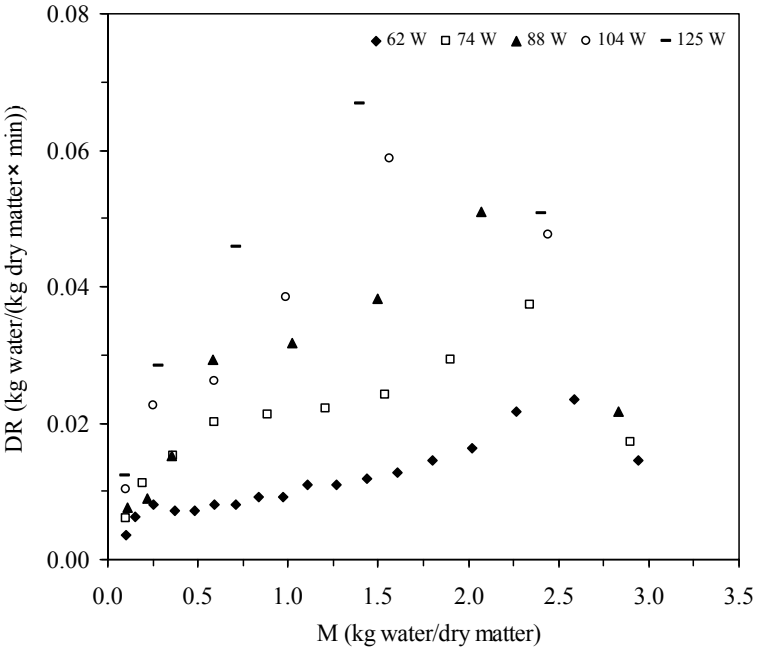

Figure 2. Drying rate as a function of moisture content at different infrared powers

3.3. Evaluation of Models

The moisture content data obtained from the drying experiments were fitted five thin-layer drying models given in Table 1. The best model selected is based on the highest R^2 and the lowest P, χ^2 and RMSE values. Results of the statistical computing are shown in Table 1. The R^2 values for all models were above 0.95. Among the five thin-layer drying models tested, Midilli and Kucuk model had the highest R^2 values and the lowest P, χ^2 and RMSE values in all the infrared drying conditions studied. It is clear that, the R^2, P, χ^2 and RMSE values of this model were changed between 0.9988-0.9999, 1.2325-2.7351, 0.000022-0.000199 and 0.005575-0.032685, respectively. Figure 3 compares experimental data with those predicted with the Midilli and Kucuk model for Jerusalem artichoke slices. As shown, the predicted moisture ratios are generally banded near to a 45° straight line, indicating the capability of the model to describe the drying behaviour of the samples appropriately. The same results have been reported in the literature in term of the Midilli and Kucuk model capability to describe the drying behaviour of different fruits and vegetables [8,26,27].

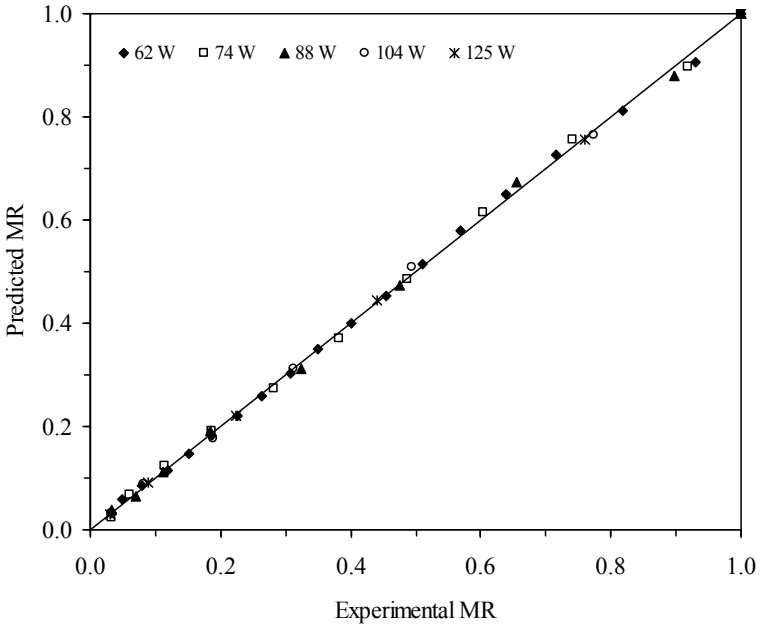

Figure 3. Experimental vs. predicted moisture ratios using Midilli and Kucuk model for different infrared powers

3.4. Effective Moisture Diffusivity

The values of effective diffusivity (D_{eff}) of Jerusalem artichoke slices were calculated using Eq. (12). The D_{eff} obtained from this study are 4.81×10^{-10}, 9.29×10^{-10}, 1.20×10^{-9}, 1.58×10^{-9} and 1.97×10^{-9} m^2/s at 62, 74, 88, 104 and 125 W, respectively. It can be seen that D_{eff} values increased greatly with increasing infrared power. Drying at 125 W has the highest value of D_{eff} and the lowest value was obtained for 62 W. The values of D_{eff} from this study lie within in general range 10^{-12} to 10^{-8} m^2/s for drying of food materials [28]. This result is similar to the results for hot-air drying of Jerusalem artichoke slices at 60-80°C [29], hot-air Jerusalem artichoke slices at 60°C [30], and microwave drying of Jerusalem artichoke slices [30].

3.5. Activation Energy

The activation energy can be determined from the slope of Arrhenius plot, *ln* (D_{eff}) versus *m/p* (Eq. (13)). The *ln* (D_{eff}) as a function of the sample weight/infrared power was plotted in Figure 4. The slope of the line is ($-E_a$) and the intercept equals to ln (D_0). The results show a linear relationship due to Arrhenius type dependence. Eq. (14) shows the effect of sample weight/infrared power on D_{eff} of samples with the following coefficients:

$$D_{eff} = 8.022\times10^{-9}\exp\left(-\frac{6746.1\ m}{p}\right) \qquad (R^2 = 0.9775) \qquad (14)$$

The estimated values of D_0 and E_a from modified Arrhenius type exponential Eq. (14) are 8.022×10^{-9} m^2/s and 6.74 kW/kg, respectively.

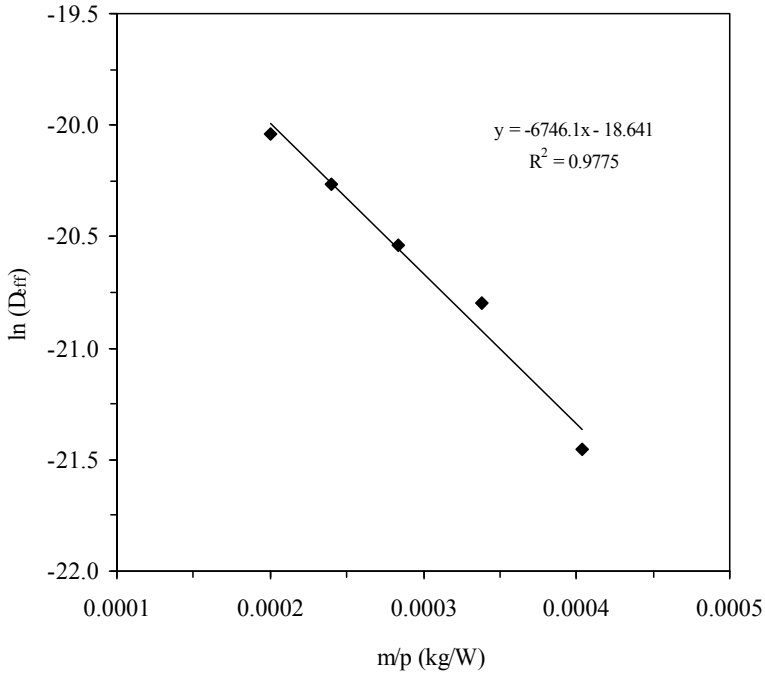

Figure 4. Arrhenius-type relationship between effective moisture diffusivity and infrared powers

3.6. Color Evaluation

Color is considered to be one of the most important criteria determining product quality and consumer preference. The results of the colour parameters fresh and obtained from the drying process are presented in Figure 5. It can be seen that all of the dried Jerusalem artichoke slices had lower values of *L* than the fresh samples. The *L* values which show lightness of product were ranged between 72.78 and 45.99. The lowest *L* value evaluated for dried product at 125 W. The decrease in *L* values might be caused by browning reactions [31]. It can be clearly seen from Figure 5, the values of a increased as the power output increased. Therefore, the samples tended toward greater redness values with the progressing drying time. On the other hand, the creation of brown pigments in the effect of non-enzymatic processes (Maillard reaction) during drying process might play an important role in the production of red color [32]. The values of b were increased with increasing of power output, indicating dried samples were yellower at high power output (high temperature).

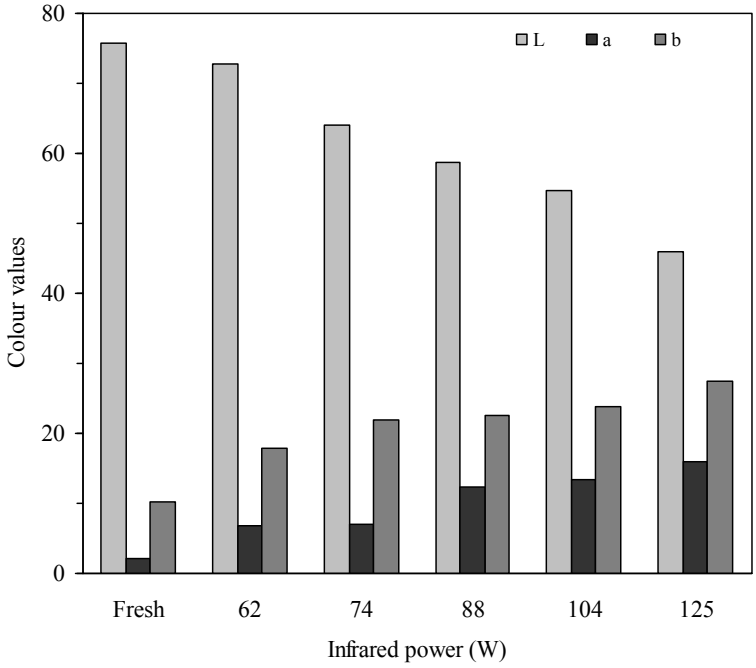

Figure 5. Colour values of Jerusalem artichoke slices fresh and dried at various infrared powers

4. CONCLUSIONS

In this study, infrared drying of Jerusalem artichoke slices was investigated. The drying rate was significantly influenced by infrared power. The drying time decreased with the increased in infrared power. The drying was observed to take place entirely in the falling rate drying period. Among five selected mathematical models, the infrared drying of Jerusalem artichoke was well represented by Midilli and Kucuk model than others. The effective moisture diffusivity was computed from Fick's second law, the values of which varied between 4.81×10^{-10} m^2/s to 1.97×10^{-9} m^2/s, over the infrared power range. With the increase of infrared power, the effective moisture diffusivity increased. The values of activation energy were estimated by a modified Arrhenius type equation and found 6.74 kW/kg.

REFERENCES

[1] Harmankaya M., Juhaimi F.A., Ozcan M.M., (2012), Mineral contents of Jerusalem artichoke (*Helianthus tuberosus* L.) growing with in Turkey, *Analytical Letters* 45, 2269-2275.

[2] Tuxtabayevna N.K., Esirgapovich S.J., (2015), Research of sorption characteristics of tubers Jerusalem artichoke (*Helianthus tuberosus*), *Food Processing & Technology*, 6(6), doi: 10.4172/2157-7110.1000453

[3] Bayraktaroglu Urun G., Yaman U.R., Kose E., (2015), Determination of drying characteristics and quality properties of eggplant in different drying conditions, *Italian Journal of Food Science*, 27, 460-467.

[4] Torki-Harchegani M., Ghanbarian D., Pirbalouti A.G., Sadeghi M., (2016), Dehydration behaviour, mathematical modelling, energy efficiency and essential oil yield of peppermint leaves undergoing microwave and hot air treatments. *Renewable and Sustainable Energy Reviews*, 58, 407-418.

[5] Touil A., Chemkhi A., Zagrouba F., (2014), Moisture diffusivity and shrinkage of fruit and Cladode of *Opuntia ficus-indica* during infrared drying, *Journal of Food Processing*, Article ID 175402, 9 Pages.

[6] Nowak D., Lewicki P.P., (2004), Infrared drying of apple slices, *Innovative Food Science & Emerging Technologies*, 5, 353-360.

[7] Sharma GP, Verma RC, Pathare PB., (2005). Thin-layer infrared radiation drying of onion slices. Journal of Food Engineering, 67: 361-366.

[8] Alaei B., Chayjan R.A., (2015), Modeling of nectarine drying under near infrared-vacuum conditions, *Acta Scientiarum Polonorum Technologia Alimentaria,* 14, 15-27.

[9] Wang J., Sheng K., (2006), Far-infrared and microwave drying of peach, *LWT-Food Science and Technology*, 39, 247-255.

[10] Shi J., Pan Z., Mchugh T.H., Wood D., Hirschberg E., Olson D., (2008), Drying and quality characteristics of fresh and sugar-infused blueberries dries with infrared radiation heating, *LWT Food Science and Technology*, 41, 1962-1972.

[11] Ertekin C, Heybeli N., (2014), Thin-layer infrared drying of mint leaves, *Journal of Food Processing and Preservation*, 38, 1480-1490.

[12] El-Beltagy A., Gamea G.R., Essa A.H.A., (2007), Solar drying characteristics of strawberry, *Journal of Food Engineering*, 78, 456-464.

[13] Erbay Z., Icier F., (2010), Thin-layer drying behaviours of olive leaves (*Olea Europaea* L.), *Journal of Food Process Engineering*, 33, 287-308.

[14] Afolabi T.J., Tunde-Akintunde T.Y., Adeyanju J.A., (2015), Mathematical modeling of drying kinetics of untreated and pretreated cocoyam slices, *Journal of Food Science and Technology*, 52, 2731-2740.

[15] Midilli A., Kucuk H., (2003), Mathematical modeling of thin layer drying of pistachio by using solar energy, *Energy Conversion and Management*, 44, 1111-1122.

[16] Arumuganathan T., Manikantan M.R., Rai R.D., Anandakumar S., Khare V., (2009), Mathematical modeling of drying kinetics of milky mushroom in a fluidized bed dryer, *International Agrophysics*, 23, 1-7.

[17] Chayjan R.A., Salari K., Abedi Q., Sabziparvar A.A., (2013), Modeling moisture diffusivity, activation energy and specific energy consumption of squash seeds in a semi fluidized and fluidized bed drying, *Journal of Food Science and Technology*, 50, 667-677.

[18] Zhang Y., Chen H., Chen, T., (2014), Drying kinetics of RDX under atmospheric pressure and vacuum conditions, *Energy Conversion and Management*, 80, 266-275.

[19] Crank J., (1975), The Mathematics of Diffusion, Oxford University Press, London, UK.

[20] Dadali G., Ozbek B., (2008), Microwave heat treatment of leek: drying kinetic and effective moisture diffusivity, *International Journal of Food Science and Technology*, 43, 1443-1451.

[21] Nasiroglu S., Kocabiyik H., (2009), Thin-layer infrared radiation drying of red pepper slices, *Journal of Food Process Engineering*, 32, 1-16.

[22] Sarimeseli A., Yuceer M., (2015), Investigation of infrared drying behaviour of spinach leaves using ANN methodology and dried product quality, *Chemical and Process Engineering*, 36, 425-436.

[23] Singh B., Panesar P.S., Nanda V., (2006), Utilization of carrot pomace for the preparation of a value added product, *World Journal of Dairy & Food Science*, 1, 22-27.

[24] Vega-Gálvez A., Miranda M., Díaz L.P., Lopez L., Rodriguez K., Di Scala K., (2010), Effective moisture diffusivity determination and mathematical modelling of the drying curves of the olive-waste cake, *Bioresource Technology*, 101, 7265-7270.

[25] Abano E.E., Ma H.L., Qu W., (2014), Thin-layer catalytic far-infrared radiation flavour of tomato slices, *Journal of Agricultural Engineering*, 45, 37-45.

[26] Akhondi E., Kazemi A., Maghsoodi V., (2011), Determination of a suitable thin layer drying curve model for saffron (*Crocus sativus* L.) stigmas in an infrared dryer, *Scientia Iranica*, 18, 1397-1401.

[27] Akpinar E.K., Toraman S., (2016), Determination of drying kinetics and convective heat transfer coefficients of ginger slices, *Heat and Mass Transfer*, 52, 2271-2281.

[28] Zogzas NP, Maroulis ZB, Marinos-Kouris D., (1996), Moisture diffusivity data compilation in foodstuffs, *Drying Technology*, 14, 2225-2253.

[29] Poorfallah Z, Nahardani M, Salaminia M, Noorian S, Mohammadi M., (2012), Kinetics of drying Jerusalem artichoke (*Helianthus tuberosus* L.) slices by hot air convective drying, *Innovation in Food Science and Technology*, 3(4), 1-12.

[30] Porniammongkol O., Duangkhamchan E., Inchuen S. (2014), Evaluation of thin-layer drying models for Jerusalem artichoke (*Helianthus tuberosus* L.) tubers in different drying models, *Suranaree Journal of Science & Technology*, 21, 47-57.

[31] Ju H.Y., El-Mashad H.M., Fang X.M., Pan Z., Xiao H.W., Liu Y.H., Gao Z.J., (2016), Drying characteristics and modeling of yam slices under different relative humidity conditions, *Drying Technology*, 34, 296-306.

[32] Vega-Galvez A., Scala K.D., Rodrguez K., Lemus-Mondaca R., Miranda M., Lopez J., Perez-Won M., (2009), Effect of air-drying temperature on physico-chemical properties, antioxidant capacity, color and total phenolic content of red pepper (*Capsicum annuum* L. var. Hungarian), *Food Chemistry*, 117, 647-653.